


Article

# Geopolymer Composites for Potential Applications in Cultural Heritage

Laura Ricciotti <sup>1,2</sup>, Antonio Jacopo Molino <sup>1,2</sup>, Valentina Roviello <sup>3</sup>, Elena Chianese <sup>4</sup> , Paola Cennamo <sup>5</sup> and Giuseppina Roviello <sup>1,2,\*</sup>

<sup>1</sup> Dipartimento di Ingegneria, Università di Napoli 'Parthenope', Centro Direzionale, Isola C4, 80143 Napoli, Italy; laura.ricciotti@uniparthenope.it (L.R.); antoniojacopo.molino@uniparthenope.it (A.J.M.)

<sup>2</sup> INSTM Research Group Napoli Parthenope, National Consortium for Science and Technology of Materials, Via G. Giusti, 9, 50121 Firenze, Italy

<sup>3</sup> Centro di Servizi Metrologici Avanzati (CeSMA), Università di Napoli 'Federico II', Corso Nicolangelo Protopisani, 80146 Napoli, Italy; valentina.roviello@unina.it

<sup>4</sup> Dipartimento di Scienze e Tecnologie, Università di Napoli 'Parthenope', Centro Direzionale, Isola C4, 80143 Napoli, Italy; elena.chianese@uniparthenope.it

<sup>5</sup> Facoltà di Lettere, Università degli Studi Suor Orsola Benincasa, Corso Vittorio Emanuele 242, 80132 Napoli, Italy; paola.cennamo@unisob.na.it

\* Correspondence: giuseppina.roviello@uniparthenope.it; Tel.: +39-081-547-6781

Received: 30 October 2017; Accepted: 8 December 2017; Published: 13 December 2017

**Abstract:** A new class of geopolymer composites, as materials alternative to traditional binders, was synthesized and its potentialities as restoration material in Cultural Heritage has been explored. This material has been prepared through a co-reticulation reaction in mild conditions of a metakaolin-based geopolymer inorganic matrix and a commercial epoxy resin. The freshly prepared slurry displays a consistency, workability and thixotropic behavior that make it suitable to be spread on different substrates in restoration, repair and reinforcement actions, even on walls and ceilings. Applicability and compatibility tests on tuff and concrete substrates were carried out and the microstructure of the samples in correspondence of the transition zone was analyzed by means of scanning electron microscope (SEM) observations and energy dispersive spectroscopy (EDS) mapping. Our studies pointed out the formation of a continuous phase between the geopolymer composite and tuff and concrete substrates, highlighting a high compatibility of the geopolymer binder with different kinds of materials. These features indicate a large potential for applications of these materials in Cultural Heritage.

**Keywords:** geopolymer; composite; Cultural Heritage

## 1. Introduction

Conservation and restoration of Cultural Heritage allows preserving and safeguarding monuments and art works for future generation. Among the causes which determine damage of artworks and Cultural Heritage, air pollution plays an important role, due to the increase in gaseous and solid pollutants concentrations in urban areas [1,2] and, consequently, in museum environments [3,4]. In general, buildings, monuments and products with heritage value require minimal and careful interventions based on surveys and diagnostic studies to find compatible materials [5]. In particular, the choice of the restoration material is dependent on several factors: the kind of chemical interaction with the substrate, interface behavior, consistency and penetration capacity, workability, adequate mechanical properties, low creeping and shrinkage, and chemical and thermal resistance. Moreover, materials used for restoration applications, besides being compatible with the original material from the chemical, physical and mechanical point of view, should present

similar aesthetic features, giving, at the same time, the opportunity to the restorer to highlight which kind of repairing action was made [5]. Finally, the restoration material should be able to adapt to the masonry movements [6,7] to avoid the risk of affecting the structural behavior of the monuments, causing collapse phenomena.

During the last decades, organic and inorganic synthetic materials have been developed to this aim focusing their application to different areas such as protective coatings, adhesive for different type of substrates (wood, wall, textiles, and ceramic), paintings, restoration and consolidation of masonry [8,9]. In detail, innovative composite materials, such as fiber-reinforced polymers, steel-reinforced grouts and textile-reinforced mortars, have been widely employed in repairing and strengthening modern and historic buildings with structural purposes [7]. Among these materials, great attention has been devoted up to now on carbon- and glass-reinforced polymers that have been widely used in the field of the Cultural Heritage thanks to their interesting mechanical and chemical properties (such as high tensile strength, stiffness-to-weight ratio, fatigue and corrosion resistance, and cost-effectiveness) of these materials. Unfortunately, the main drawbacks in the use of these systems are their brittle failure and sensitivity to impact, notching and environmental agents.

In this framework, a highly promising class of inorganic materials alternative to traditional binders are geopolymers [10,11], which are amorphous materials obtained from the alkaline activation of an aluminosilicate source in a silicate solution. This reaction yields to a three-dimensional framework in which  $\text{SiO}_4$  and  $\text{AlO}_4$  tetrahedra are linked by corner-shared O atoms.

Geopolymers are characterized by interesting mechanical properties, low shrinkage, thermal stability, freeze–thaw, chemical and fire resistance, long term durability and recyclability. Thus, they can be used in place of Ordinary Portland Cement (OPC) in a wide range of applications, such as fireproof barriers, materials for high temperatures, matrices for hazardous waste stabilization, toolings and moldings [12–14]. Besides, the use of geopolymer-based materials in concrete applications could significantly reduce the  $\text{CO}_2$  emissions [15] thanks to the “low carbon” footprint of several raw materials with a high concentration of aluminosilicates from which they can be prepared, e.g., dehydroxylated kaolinite (metakaolin, MK) or industrial waste such as fly ash. Unfortunately, it should be pointed out that geopolymer slurries are characterized by poor rheological properties since they tend to drain due to a low viscosity that strongly limit their applicability in restoration works, in particular on vertical masonry or artefact.

Recently, to modify suitably the mechanical, physical and chemical properties of these systems, organic–geopolymer binders have been synthesized by means of a reaction of co-reticulation that takes place between the organic phase (epoxy resin precursors or polysiloxane oligomers) and the inorganic one [16–20]. These materials have shown widely tunable performance depending on their composition and reaction conditions with significant potential applications in the fields of structural, fire-resistant and insulating applications [21–29]. As far as their rheological behavior, it is worth pointing out that the addition of the organic resin into the geopolymeric slurry causes a significant change in the intrinsic viscosity of the whole system, thus allowing the obtainment of a homogeneous and workable thixotropic mixture [27], easy to model in different shapes and to be spread also on vertical substrates.

The present paper reports on the preparation and characterization of geopolymer-based composites containing a limited content (up to 10% by weight) of a commercial epoxy resin and their use as potential repairing materials for different systems (tuff and cement-based materials). Moreover, to reduce the drying shrinkage of the material so favoring its adhesion to the investigated substrates, the composition of the geopolymer composites has been modified by addition of marble powder. The samples have been cured at room temperature to simulate outdoor conditions and subjected to morphological, thermal, rheological, physico-chemical and mechanical characterizations. In particular, aiming at the study of the compatibility, binding, protective and repair efficiency of the geopolymer-based composite with the substrates, detailed microstructural analyses and energy dispersive spectroscopy (EDS) mapping have been performed by means of scanning electron microscopy on the interfacial transition zone between the geopolymeric matrix and the substrates.

In addition, to consider the release of ionic compounds after the contact with aqueous solutions simulating the behavior in presence of atmospheric humidity, geopolymer samples were washed with ultrapure water and the obtained solutions were analyzed by determining pH and ionic composition.

## 2. Materials and Methods

### 2.1. Materials

Metakaolin (MK) was kindly provided by Neuchem S.r.l. (Milan, Italy). Sodium hydroxide with reagent grade, was supplied by Sigma-Aldrich. The sodium silicate solution (SS) was supplied by Prochin Italia S.r.l (Caserta, Italy). Waste marble slurry was dried at 105 °C for 4 h and milled to produce marble powder (MP) with particle sizes ranging between 10 and 300 µm. The composition of metakaolin, sodium silicate solution and marble powder are shown in Table 1. The epoxy resin used in this paper, called Epojet<sup>®</sup>, was purchased by Mapei S.p.A (Milan, Italy): it is a commercial two-component epoxy adhesive for injection, which, after the mixing, takes the aspect of a low viscosity liquid and it is usable for 40 min at room temperature (see Ref. [19] for additional experimental details).

**Table 1.** Chemical composition (weight %) of the metakaolin (MK), marble powder (MP) and sodium silicate solution (SS).

Sample	Metakaolin	Marble Powder	Sodium Silicate
SiO <sub>2</sub>	52.90	1.12	27.40
Al <sub>2</sub> O <sub>3</sub>	41.90	0.37	-
CaO	0.17	52.26	-
Fe <sub>2</sub> O <sub>3</sub>	1.60	0.11	-
MgO	0.19	0.87	-
K <sub>2</sub> O	0.77	0.10	-
Na <sub>2</sub> O	-	0.14	8.15
Water	-	-	64.45
LoI *	2.47	45.03	-

\* LoI = Loss on Ignition.

### 2.2. Sample Preparation

#### 2.2.1. Geopolymer (GMK)

The alkaline activating solution was prepared by dissolving solid sodium hydroxide into the sodium silicate solution. The solution was then allowed to equilibrate and cool for 24 h. The composition of the solution can be expressed as Na<sub>2</sub>O·1.4SiO<sub>2</sub>·10.5H<sub>2</sub>O. Metakaolin was then incorporated into the activating solution with a liquid to solid ratio of 1.4:1 by weight, and mixed by hand for 10 min. The composition of the whole geopolymeric system can be expressed as Al<sub>2</sub>O<sub>3</sub>·3.5SiO<sub>2</sub>·1.0Na<sub>2</sub>O·10.5H<sub>2</sub>O, corresponding to a complete geopolymerization process, as revealed by EDS analysis on the cured samples. The neat geopolymer sample was indicated as GMK.

#### 2.2.2. Geopolymer Composites (GMK-E and GMK-E-MP)

Geopolymer-based composite GMK-E was obtained by adding 10% by weight of Epojet<sup>®</sup> resin to the freshly-prepared geopolymeric suspension, and quickly incorporated by hand mixing (10 min; see Ref. [19] for additional experimental details).

Before being added to the geopolymeric mixture, Epojet<sup>®</sup> was cured at room temperature for 10 min, when it was still easily workable and long before its complete crosslinking and hardening (that takes place in about 5–7 h at 23 °C). Instead, GMK-E-MP was synthesized by adding the marble powder to geopolymer composite slurry and the obtained mixture was stirred by hand mixing for 5 min. The composites presented a homogeneous aspect and started solidifying in few minutes. The mix design details of the specimens are reported in Table 2.

**Table 2.** Composition (weight %) of the materials designed in this study.

Sample	MK	SS	NaOH	Resin	MP
GMK	41.6	50.0	8.4	-	-
GMK-E	37.4	45.0	7.6	10	-
GMK-E-MP	30.0	36.0	6.0	8.0	20.0

### 2.2.3. Curing Treatments

All the specimens, as soon as prepared, were poured in cubic molds ( $40 \times 40 \times 40 \text{ mm}^3$ ) and cured in >95% relative humidity conditions at room temperature for 7 days and further 21 days in air (see Ref. [19] for additional experimental details). The evaporation of water was prevented by sealing the top of the molds with a thin plastic layer during storage as well as during the curing stage.

## 2.3. Geopolymers Characterization Methods

### 2.3.1. Thermogravimetric Analysis (TGA)

Thermogravimetric analyses were performed by a TA Instrument SDT2960 simultaneous DSC-TGA. The thermographs were obtained at a heating rate of  $10 \text{ }^\circ\text{C}/\text{min}$  using  $\approx 10 \text{ mg}$  of the powdered sample under air flow, with a temperature range  $25\text{--}800 \text{ }^\circ\text{C}$ .

### 2.3.2. Fourier Transform Infrared Spectroscopy (FT-IR)

FT-IR measurements were performed using a Jasco FT/IR-430 spectrometer. As far as the geopolymer and composite samples, the experiments were carried out by using KBr discs in which few milligrams of the already cured specimens were dispersed. Otherwise, the organic resin was analyzed by using free standing thin films.

### 2.3.3. X-ray Powder Diffraction (XRD)

Wide-angle X-ray diffraction patterns were obtained at room temperature with nickel-filtered  $\text{Cu K}\alpha$  radiation with an automatic Philips powder diffractometer operating in the  $\theta/2\theta$  Bragg-Brentano geometry using specimen holders of thickness equal to 2 mm. The phase recognition was carried out by using the PDF-4+ 2012 (ICDD—International Centre for Diffraction Data<sup>®</sup>, 12 Campus Blvd., Newtown Square, PA, USA) database and the HighScore Plus (Malvern Panalytical B.V., Eindhoven, The Netherlands) software.

### 2.3.4. Compressive Strength Test

The compressive strength of the geopolymer and composite specimens was measured by testing cubic specimens ( $40 \times 40 \times 40 \text{ mm}^3$ ) in a Controls MCC8 compression-testing machine (2000 kN) (Controls, Cernusco s/N., Milan, Italy). The compressive strength was calculated from the failure load divided by the cross-sectional area resisting the load and reported in MPa. The values reported are the averages of the three compressions strength values.

### 2.3.5. SEM Analysis

SEM analysis was carried out by means of a Phenom Pro X Microscope (Phenom-World B.V., Eindhoven, The Netherlands) on the surface of the samples and on their fresh fracture surfaces after a gold layer deposition by means of metallization process. The acceleration voltage was in the range  $5\text{--}15 \text{ kV}$ . The energy dispersive X-ray spectrometer (Phenom-World B.V., Eindhoven, The Netherlands) has the following specifications: silicon drift detector, thermoelectrically cooled ( $\text{LN}_2$  free); the X-ray window has ultra-thin silicon nitride ( $\text{Si}_3\text{N}_4$ ) operating with  $\text{Mn K}\alpha \leq 137 \text{ eV}$  energy resolution.

### 2.3.6. Rheological Measurement

Simple flow measurements related to pastes can be performed by means of the minislump cone test. In this work, the geometry of the minislump cone was as follows: top diameter equal to 5.0 cm; bottom diameter equal to 6.8 cm; height equal to 6.5 cm (corresponding to a paste volume equal to 179.1 cm<sup>3</sup>). Freshly prepared slurries were slowly poured in the cone placed on a horizontal plane and carefully compacted by means of a thin steel rod. Slump orthogonal diameters were measured and the average diameter was used to calculate minislump area. Mini-slump measurements were repeated at 0, 15, 30, 60 and 120 min to enlighten workability loss depending on time, by keeping the fresh slurries in controlled environment ( $T = 20 \pm 2$  °C; sealed container). Apparent viscosity of geopolymeric mixtures was assessed by means of a Brookfield viscometer DV2T. Test were carried out with different spindles considering the variation of rheological features of investigated mixtures. The used spindles were standardized for the indicated device and were indicated by numbers, namely n° 4, 5, 6 and 7.

### 2.3.7. Determination of the Water-Soluble Salt Content

To assess the release of ionic compounds when in contact with water solutions, geopolymer materials were treated with ultrapure water.

Moreover, to evaluate the relation between ion release and weight and thickness of material, two specimens were used, with weight of 12.8156 g and 20.9726 g and a thickness of 3 mm and 6 mm, indicated as A and B, respectively.

Each sample was treated with 50 mL of ultrapure water and maintained in contact with the solution for one week; after this period the solution was recovered, filtered at 0.2 µm and analyzed for ion content and pH values, repeating the washing process four times.

Ion content was determined by using a Dionex System ICS1100, equipped with two parallel systems for cation and anion detection. For anion measurements, a cell volume of 100 µL, a tampon solution 3.5 mM of sodium carbonate/sodium bicarbonate as eluent and a flow rate of 1.20 mL/min were used.

Calibration curves were implemented by dilution starting by certified multistandard solutions containing Cl<sup>-</sup>, F<sup>-</sup>, Br, NO<sub>2</sub><sup>-</sup>, NO<sub>3</sub><sup>-</sup>, PO<sub>4</sub><sup>3-</sup>, SO<sub>4</sub><sup>2-</sup> as inorganic species and HCOO<sup>-</sup>, CH<sub>3</sub>COO<sup>-</sup> and C<sub>2</sub>O<sub>4</sub><sup>2-</sup> as organic species.

For cation detection, a cell volume of 25 µL, a solution of methanesulfonic acid 20 mM as eluent and a flow rate of 0.25 mL/min were used; as for anions, calibration curves were implemented by dilution starting by certified multistandard solutions containing: Li<sup>+</sup>, Na<sup>+</sup>, K<sup>+</sup>, NH<sub>4</sub><sup>+</sup>, Ca<sup>2+</sup>, Mg<sup>2+</sup>.

For pH measurements, a pH/ion meter 781 Metrohm was used.

## 3. Results and Discussion

### 3.1. Material Characterization

#### 3.1.1. Thermal Analysis (TGA)

Thermogravimetric analyses were performed on the unmodified geopolymer GMK, on the organic resin and on the GMK-E composite, to compare their thermal behavior after curing at room temperature for seven days in 99% relative humidity conditions. The corresponding curves are shown in Figure 1.

As far as GMK sample, the weight loss starts at  $\approx 30$  °C with maximum weight loss temperature around 120–130 °C and is completed at  $\approx 500$  °C. This loss can be attributed to the removal of water molecules absorbed (up to  $\approx 100$  °C) or differently linked (up to  $\approx 200$  °C, free water in the pores; at higher temperatures, structural water and bound water in the nanopores) to the silicate molecules [30].

Instead, the organic resin and GMK-E composite show a degradation mechanism involving two main steps. Particularly, as regards the resin, the thermogram shows a thermal stability up to about 250 °C. Above this temperature, a first degradation step that finishes at  $\approx 480$  °C is observed,

resulting in a weight loss of 51%. The second degradation process is completed at about 650 °C and no combustion residual remains.

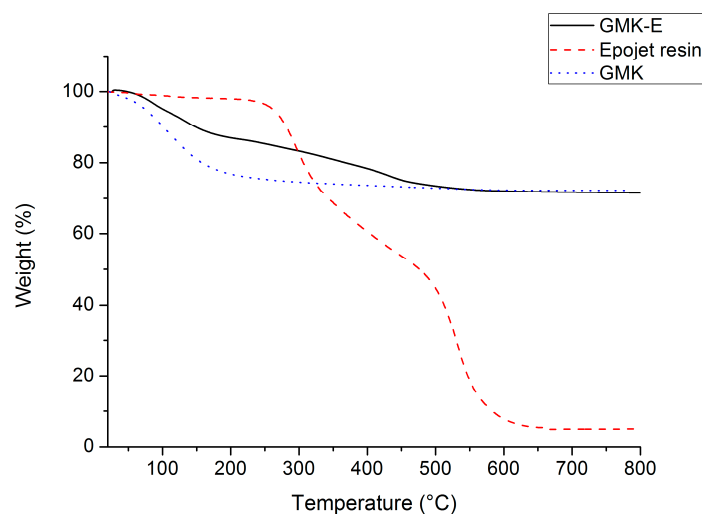


**Figure 1.** TGA curves of GMK-E composite (black continuous line), Epojet<sup>®</sup> resin (red dashed line) and GMK sample (blue dotted line).

As far as G-MK-E composite, a first step, corresponding to a weight loss of  $\approx 10\%$ , is recorded up to  $\approx 150$  °C, while a second step is observed up to  $\approx 600$  °C and corresponds to a further weight loss equal to  $\approx 20\%$ . From the comparison of the TGA curves of the neat geopolymer and of the epoxy resin (see Figure 1), it is possible to associate the first degradation step mainly with the loss of water of the geopolymeric phase while the remaining one corresponds to the degradation of the dispersed organic phase. The combustion residual at 800 °C is about 70%.

Moreover, it is worth pointing out that the weight loss for the composite occurs at higher temperature value if compared to that of the pure geopolymer: probably the polar groups of the resin interact with the water molecules delaying their evaporation.

Degradation temperatures and weight losses for all the studied systems are summarized in Table 3.

**Table 3.** Thermal properties of the neat geopolymer, epoxy resin and composite sample.

Sample	Wt <sub>s</sub> (°C) <sup>1</sup>	Wt <sub>e</sub> (°C) <sup>2</sup>	R (Weight %) <sup>3</sup>
GMK	30	500	72
GMK-E	30	600	70
Epojet <sup>®</sup> resin	250	650	0

<sup>1</sup> Wt<sub>s</sub>: weight loss starting temperature (°C); <sup>2</sup> Wt<sub>e</sub>: weight loss ending temperature (°C); <sup>3</sup> R: residual at 800 °C (weight %).

### 3.1.2. FT-IR Analysis

The FT-IR spectra of the GMK geopolymer, the organic resin and of GMK-E composite are shown in Figure 2.

The FTIR spectrum of the geopolymer (Figure 2, curve a) shows broad bands at about 3440 cm<sup>-1</sup> and 1630 cm<sup>-1</sup> due to O-H stretching and bending modes of absorbed molecular water [31,32] and a strong band at about 1035 cm<sup>-1</sup> due to Si-O stretching vibrations [32]. Moreover, the signal at about 460 cm<sup>-1</sup> is due to Si-O bending vibration [31–38].

As far as the FT-IR spectrum of Epojet<sup>®</sup> (Figure 2, curve b), the presence of the broad band at  $\approx 3400$  cm<sup>-1</sup> is assigned to O-H stretching of hydroxyl group [37]. The signals in the wavenumber range 2968–2854 cm<sup>-1</sup> and about 1460 cm<sup>-1</sup> are due to -CH<sub>2</sub>- symmetric and asymmetric stretching

and bending, respectively [36]. Moreover, signals located in the range  $1300\text{--}1050\text{ cm}^{-1}$  can be assigned to C-C and C-O stretching [36]. In addition, it is possible to observe different bands that are due to aromatic rings: C-H stretching at about  $3030\text{ cm}^{-1}$ , C-H and C=C bending in the wavenumber ranges  $860\text{--}680$  and  $1700\text{--}1500\text{ cm}^{-1}$  respectively. Concerning the geopolymer-based composite, its spectrum (Figure 2, curve c) is characterized by the main bands of pure organic resins and of the inorganic geopolymer. In particular, the broad bands at about  $3435\text{ cm}^{-1}$  and  $1630\text{ cm}^{-1}$  are due to O-H stretching and bending modes of absorbed molecular water while the band at  $1040\text{ cm}^{-1}$  is due to Si-O stretching and that at about  $460\text{ cm}^{-1}$  is due to Si-O bending vibration. Finally, the bands in the region  $800\text{--}600\text{ cm}^{-1}$  are associated to Si-O-Al vibrations [39–43].

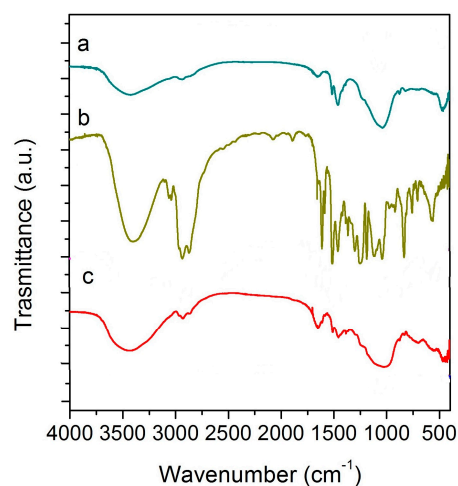


**Figure 2.** Fourier Transform Infrared Spectroscopy (FT-IR) spectra of: (a) geopolymer; (b) Epojet<sup>®</sup> resin; and (c) GMK-E composite.

### 3.1.3. X-ray Diffraction Characterization

Figure 3 shows the X-ray powder diffraction patterns of: the unreacted metakaolin (a); the neat geopolymer GMK (b); and the composite GMK-E (c).

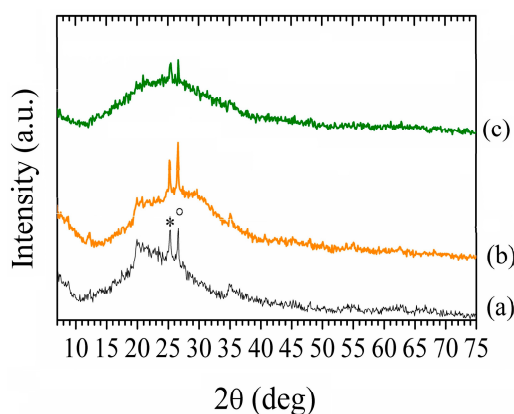


**Figure 3.** X-ray powder diffraction patterns of: (a) metakaolin; (b) Geopolymer GMK; and (c) GMK-E composite. \* = anatase; ° = quartz.

As apparent, the diffraction pattern of the metakaolin specimen (Figure 3, line a) used for the preparation of the geopolymeric sample reveals that it is predominantly amorphous, being characterized by the presence of a large halo centered at  $2\theta \approx 20\text{--}25^\circ$  and by some minor diffraction peaks revealing the presence of residual kaolinite ( $2\theta \approx 19\text{--}21^\circ$ ) and small impurities

probably represented by anatase (diffraction peak at  $25.3^\circ$ ) and quartz (the strong peak at  $27.5^\circ$ ). In line with what is usually observed for samples prepared in similar conditions and with similar composition, the major feature of XRD powder diffraction patterns of the geopolymer (Figure 3, line b) is a largely featureless “hump” centered at approximately  $27^\circ$ – $29^\circ$ . In addition, GMK-E specimen (Figure 3, line c) appears amorphous.

### 3.1.4. Compressive Strength Test

The compressive strengths of GMK and GMK-E samples cured for 28 days are reported in Figure 4. As evident, the incorporation of the organic resin in the neat geopolymeric material significantly influences its mechanical properties, resulting in an increase of the compressive strength with respect to GMK sample. This improvement is probably due to the presence of the organic phase that acts as reinforcement, thanks to a crack deviation mechanism and absorbing part of the load by plastic deformation [19].

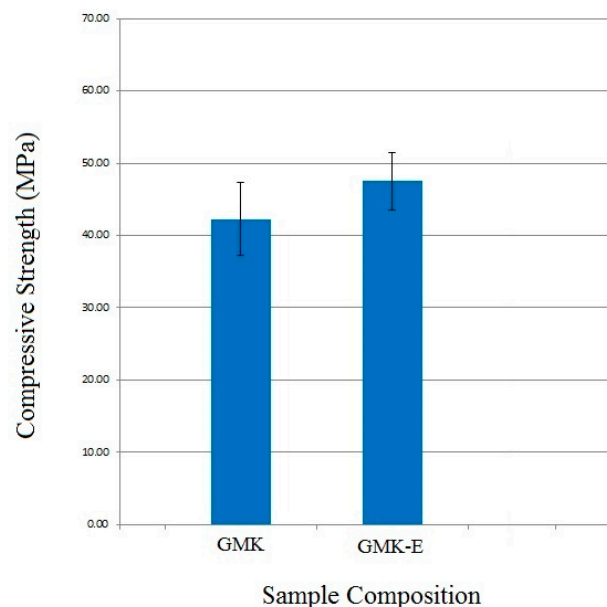


**Figure 4.** Compressive Strength (MPa) of the GMK and GMK-E samples.

### 3.1.5. Textural and Microstructural Characterizations

Figure 5 shows some pictures of the geopolymer composite slurry before its consolidation.

As highlighted by means of slump and rheological tests, it is apparent that the slurry is characterized by a good viscosity that make it suitable for applications on several substrates such as tuff and concrete.

Slump test results are reported in Figure 6 and refer to the GMK and GMK-E slurries tested as soon as prepared and for different resting times. The system exhibiting the largest flow is GMK, while GMK-E could keep almost unchanged the shape of the slump cone after cone lifting due to very high values of viscosity and yield stress, thus indicating a strongly different rheological performance with respect to earlier investigated material. In terms of workability loss, the GMK system could keep its characteristic flow area for at least 30 min. Instead, GMK-E did not experience any significant change over time since the starting value of mini slump area, which was substantially similar to the bottom area of the cone, was kept almost constant for all subsequent measurements.





**Figure 5.** GMK-E composite as soon as obtained by hand mixing (A); and some qualitative test of adhesion and thixotropic behavior on: (B) concrete; and (C,D) tuff. See Ref. [19,27] for details.

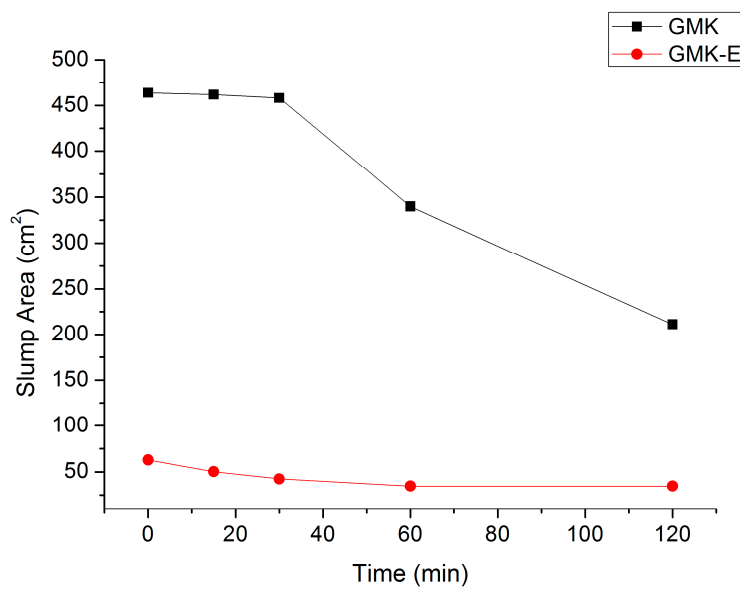


**Figure 6.** Variation of slump area with time for GMK (black squares) and GMK-E (red circles) slurries.

Apparent viscosity measurements related to GMK and GMK-E slurries are reported in Figure 7. The measurements were performed with different rotating spindles to provide further information and ensure a better reproducibility of the results. The possibility of using several spindles depends on the viscosity of the investigated suspension: for relatively high viscosity values, the number of suitable spindles is limited. In Figure 7, it is evident that GMK-E is characterized by higher viscosity than GMK.

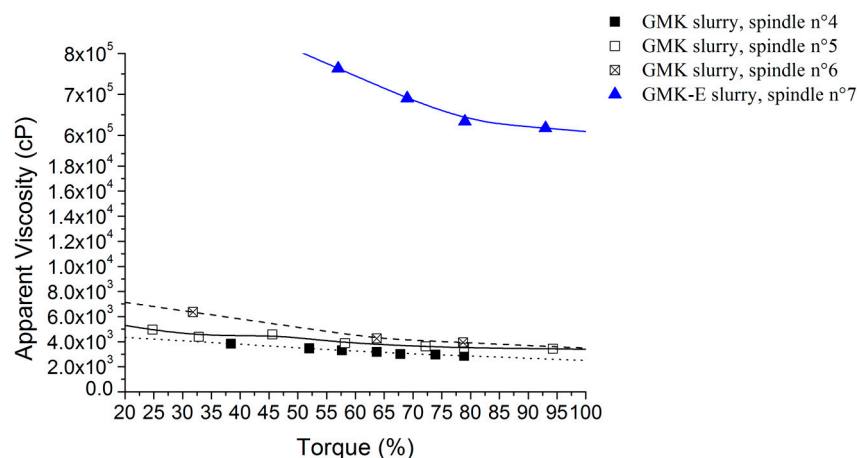


**Figure 7.** Apparent viscosity of GMK (squares) and GMK-E (triangles) slurries as measured with the spindle indicated.

As far as the apparent viscosity of the GMK-E slurry, the measurement was strongly influenced by the applied shear regime. In particular, for the GMK-E slurry, an apparent viscosity equal to  $6.8 \times 10^5 \pm 0.4 \times 10^5$  cP was measured.

Moreover, it is worth pointing out that right after its preparation, the composite slurry shows a very good tixotropic behavior allowing its application on vertical walls and ceilings.

To explore the potential use of GMK-E composite as fixing and reinforcing material, the interfaces between different substrates and cured GMK-E have been characterized in detail by means of SEM observations and EDS mapping (Figure 8) in which also the characterization of the sample GMK-E-MP is reported. It is worth recalling that this last sample (containing also marble powder) was prepared aiming at reducing the shrinkage of the binder, thus favoring a better adhesion with the analyzed substrates. As apparent, GMK-E shows a very good homogeneity and uniformity of the micro dispersion of well-defined organic particles into the inorganic matrix (Figure 8A): in particular, resin particles are in the range of 1–10  $\mu\text{m}$  and no agglomeration phenomena can be observed. Moreover, a very strict adhesion between the organic and inorganic phases can be observed, so strong that the particles of resin are scratched when the specimens are broken to prepare the SEM samples. At variance, the GMK-E-MP sample (Figure 8B) shows a different morphology due to the presence of  $\text{CaCO}_3$  particles: in this sample, the structure appears to be less compact, grainy and porous, due to the presence of several grains with dimensions of a few micron, that characterizes the inorganic matrix, while the organic phase appears once again of spherical shape and well dispersed in the inorganic matrix.

The morphologies of the tuff and concrete substrates are shown in Figure 8C,D, respectively. In particular, the tuff sample shows a grainy and porous structure, while the concrete sample shows a quite compact structure.

Figure 8E,G shows the interface transition zone between the GMK-E-MP sample (lower part of the figures) and the tuff and concrete substrates (upper part of the figures), respectively. As also confirmed by EDS maps, carried out in the same transition zones (Figure 8F shows the transition zone with the tuff substrate, while Figure 8H shows that one with the concrete substrate), the geopolymer composite and the two different substrates seem to form a continuous phase, with no neat interface and fractures. This very continuous morphology is a consequence of the high compatibility between the geopolymer composite and the substrates.

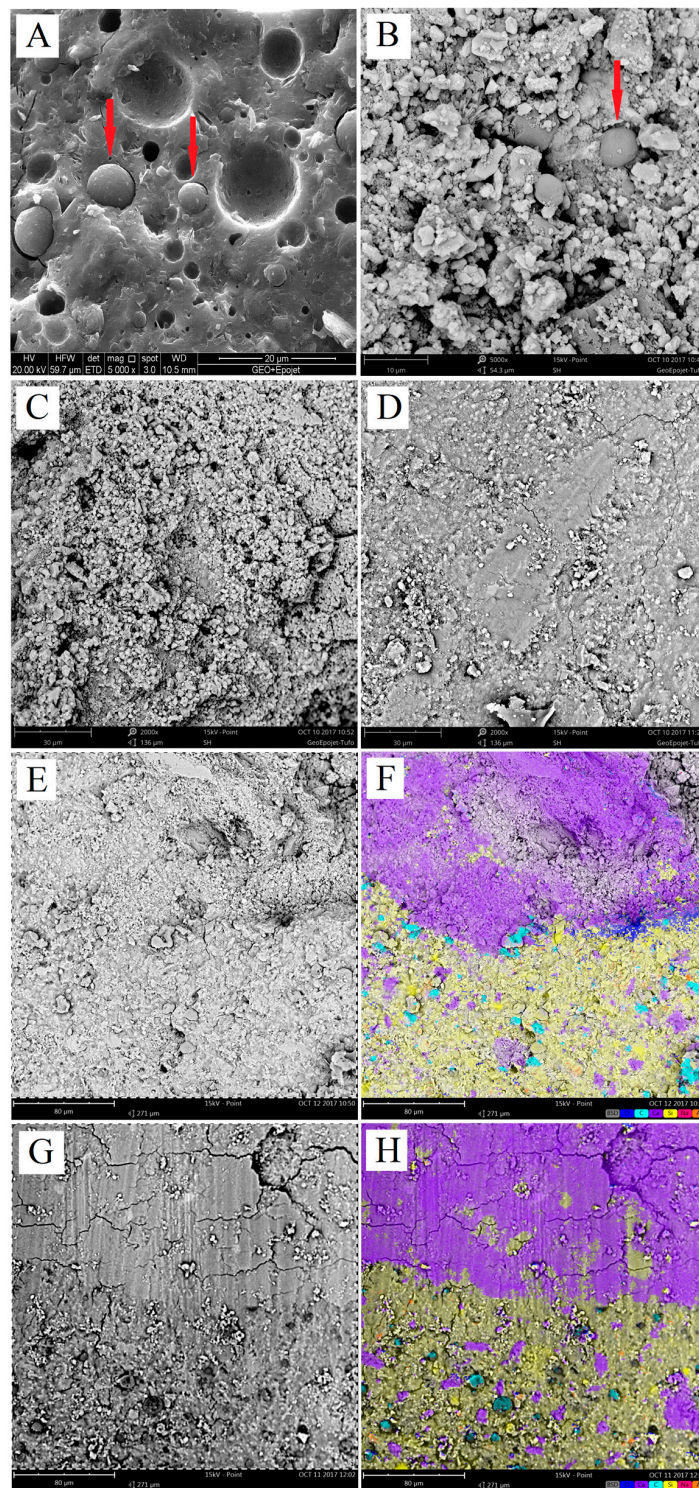


**Figure 8.** scanning electron microscope (SEM) micrographs of fracture surface of: GMK-E (A); GMK-E-MP(B); tuff (C); concrete (D); and of the interface transition zone: between GMK-E-MP and tuff substrate (E); and between GMK-E-MP and concrete substrate (G). (F,H) EDS maps of the interface transition zone GMK-E-MP/tuff and GMK-E-MP/concrete substrate are shown, respectively: the presence of Ca atoms, characterizing the chemical composition of tuff and concrete substrates, is evidenced by purple color while that one of Si atoms, characterizing the geopolymer phase, is highlighted in yellow. The red arrows indicate the epoxy resin particles.

### 3.1.6. Determination of the Water-Soluble Salt Content

Ionic composition and pH values of the solutions obtained after washing are shown in Table 4.

**Table 4.** Ionic composition and pH values of the washing solutions.

Sample <sup>1</sup>	F <sup>-</sup> (mg/ (g Sample))	Cl <sup>-</sup> (mg/ (g Sample))	NO <sub>3</sub> <sup>-</sup> (mg/ (g Sample))	PO <sub>4</sub> <sup>3-</sup> (mg/ (g Sample))	SO <sub>4</sub> <sup>2-</sup> (mg/ (g Sample))	Na <sup>+</sup> (mg/ (g Sample))	K <sup>+</sup> (mg/ (g Sample))	pH
GMK-E-AI	0.020	0.106	0.027	0.056	0.266	6.701	0.100	11.1
GMK-E-BI	0.017	0.077	0.013	0.023	0.173	5.518	0.069	10.6
GMK-E-AII	0.004	0.028	0.011	0.016	0.047	1.661	0.045	10.5
GMK-E-BII	0.004	0.017	0.007	0.013	0.040	1.634	0.025	10.4
GMK-E-AIII	0.000	0.016	0.011	0.011	0.030	1.260	0.044	9.8
GMK-E-BIII	0.000	0.016	0.007	0.008	0.031	1.108	0.032	10.1
GMK-E-AIV	0.000	0.005	0.011	0.010	0.021	0.736	0.031	10.0
GMK-E-BIV	0.000	0.005	0.007	0.007	0.022	0.726	0.019	10.2

<sup>1</sup> For each measurement, two specimens were used, in which a weight of 12.8156 g and 20.9726 g and a thickness of 3 mm and 6 mm were used, indicated as A and B, respectively. Roman numbers indicate the subsequent washings carried out on GMK-E.

Ion concentrations were expressed as mg of ion per g of sample; bromine, nitrite, formiate, acetate, ossalate, calcium, ammonium, and magnesium were always below detection limits. As expected, due to starting raw materials used for geopolymer synthesis, the most abundant ion was sodium, which presented a concentration, after first washing, corresponding to 6.701 mg/g for sample A, with minor thickness, and 5.518 for sample B, with major thickness. A little difference between samples A and B was observed in each washing stage, with higher ion release for the firsts ones; after second washing step, concentrations decreased several times becoming comparable between samples A and B and becoming compatible for the use in Cultural Heritage consolidation [11].

pH values were always high, diminishing of one point after four washing steps; this means that geopolymer maintains alkaline characteristics in the medium, resulting compatible with great part of supports used in Cultural Heritage [11].

For all measured ions, the measured concentrations were negligible or were reduced after a few number of washing steps and with a limited consumption of water if compared to the initial sample weight.

## 4. Conclusions

A preliminary investigation of the potentialities of geopolymer-based composites as restoration material in the field of Cultural Heritage has been carried out. This study shows that the composite geopolymeric slurry is characterized by a high workability and very good thixotropic behavior, which makes it easy to spread and model on different substrates commonly used in the field of restoration. Moreover, the chemical compatibility of the composite material with the substrates ensures a good adhesion with them, highlighting the possibility of using this kind of binder as fixing and joining material.

Chemical compatibility was also assessed by measuring the release of ionic species after contact with water; the obtained results showed a little amount of ion charge with respect to weight of the tested geopolymer and a restrained dependence on sample thickness.

Finally, it is worth noting that the geopolymer composites slurry can be easily colored by simply adding pigments to fulfill the requirements of restorer needs.

**Acknowledgments:** Acknowledgements are due to Neuvendis S.p.A. for the metakaolin supply and Prochin Italia S.r.l. for the silicate solution supply. Luciana Cimino and Giovanni Morieri are warmly acknowledged for assistance in laboratory activities.

**Author Contributions:** Laura Ricciotti, Elena Chianese and Giuseppina Roviello conceived and designed the experiments. Laura Ricciotti, Antonio Jacopo Molino and Valentina Roviello carried out the experimental work. Laura Ricciotti, Elena Chianese, Paola Cennamo and Giuseppina Roviello analyzed the data. Laura Ricciotti and Giuseppina Roviello wrote the paper.

**Conflicts of Interest:** The authors declare no conflict of interest.

## References

1. Riccio, A.; Chianese, E.; Agrillo, G.; Esposito, C.; Ferrara, L.; Tirimberio, G. Source apportionment of atmospheric particulate matter: A joint Eulerian/Lagrangian approach. *Environ. Sci. Pollut. Res.* **2014**, *21*, 13160–13168. [[CrossRef](#)] [[PubMed](#)]
2. Riccio, A.; Chianese, E.; Tirimberio, G.; Prati, M.V. Emission factors of inorganic ions from road traffic: A case study from the city of Naples (Italy). *Transp. Res. Part D Transp. Environ.* **2017**, *54*, 239–249. [[CrossRef](#)]
3. Chianese, E.; Riccio, A.; Duro, I.; Trifuoggi, M.; Iovino, P.; Capasso, S.; Barone, G. Measurements for indoor air quality assessment at the Capodimonte Museum in Naples (Italy). *Int. J. Environ. Res.* **2012**, *6*, 509–518.
4. Ozga, I.; Ghedini, N.; Giosuè, C.; Sabbioni, C.; Tittarelli, F.; Bonazza, B. Assessment of air pollutant sources in the deposit on monuments by multivariate analysis. *Sci. Total Environ.* **2014**, *490*, 776–784. [[CrossRef](#)] [[PubMed](#)]
5. International Council on Monuments and Sites (ICOMOS); International Scientific Committee for Analysis and Restoration of Structures of Architectural Heritage. *Recommendations for the Analysis, Conservation and Structural Restoration of Architectural Heritage*; ICOMOS: Paris, France, 2003.
6. Corradi, M.; Tedeschi, C.; Binda, L.; Borri, A. Experimental evaluation of shear and compression strength of masonry wall before and after reinforcement: Deep repointing. *Constr. Build. Mater.* **2008**, *22*, 463–472. [[CrossRef](#)]
7. Valluzzi, M.R.; Modena, C.; de Felice, G. Current practice and open issues in strengthening historical buildings with composites. *Mater. Struct.* **2014**, *47*, 1971–1985. [[CrossRef](#)]
8. Bergamonti, L.; Alfieri, I.; Lorenzi, A.; Predieri, G.; Barone, G.; Gemelli, G.; Mazzoleni, P.; Raneri, S.; Bersani, D.; Lottic, P.P. Nanocrystalline TiO<sub>2</sub> coatings by sol-gel: Photocatalytic activity on Pietra di Noto biocalcarene. *J. Sol-Gel Sci. Technol.* **2015**, *75*, 141–151. [[CrossRef](#)]
9. Cocca, M.; D'Arienzo, L.; D'Orazio, L.; Gentile, G.; Martuscelli, E. Polyacrylates for conservation: Chemico-physical properties and durability of different commercial products. *Polym. Test.* **2004**, *23*, 333–342. [[CrossRef](#)]
10. Clausi, M.; Tarantino, S.C.; Magnani, L.L.; Riccardi, M.P.; Tedeschi, C.; Zema, M. Metakaolin as a precursor of materials for applications in Cultural Heritage: Geopolymer-based mortars with ornamental stone aggregates. *Appl. Clay Sci.* **2016**, *132–133*, 589–599. [[CrossRef](#)]
11. Geraldès, C.F.M.; Lima, A.M.; Delgado-Rodrigues, J.; Mimoso, J.M.; Pereira, S.R.M. Geopolymers as potential repair material in tiles conservation. *Appl. Phys. A* **2016**, *122*, 197. [[CrossRef](#)]
12. Rowles, M.; O'Connor, B. Chemical optimisation of the compressive strength of aluminosilicate geopolymers synthesised by sodium silicate activation of metakaolinite. *J. Mater. Chem.* **2003**, *13*, 1161–1165. [[CrossRef](#)]
13. Davidovits, J. *Geopolymer Chemistry and Applications*, 3rd ed.; Institut Geopolymere: Saint Quentin, France, 2011.
14. Habert, G.; Ouellet-Plamondon, C. Recent update on the environmental impact of geopolymers. *RILEM Tech. Lett.* **2016**, *1*, 17–23. [[CrossRef](#)]
15. Duxson, P.; Provis, J.L.; Lukey, G.C.; Van Deventer, J.S. The role of inorganic polymer technology in the development of 'green concrete'. *Cem. Concr. Res.* **2007**, *37*, 1590–1597. [[CrossRef](#)]
16. Ferone, C.; Roviello, G.; Colangelo, F.; Cioffi, R.; Tarallo, O. Novel hybrid organic-geopolymer materials. *Appl. Clay Sci.* **2013**, *73*, 42–50. [[CrossRef](#)]
17. Ferone, C.; Colangelo, F.; Roviello, G.; Asprone, D.; Menna, C.; Balsamo, A.; Manfredi, G. Application-oriented chemical optimization of a metakaolin based geopolymer. *Materials* **2013**, *6*, 1920–1939. [[CrossRef](#)] [[PubMed](#)]
18. Ricciotti, L.; Roviello, G.; Tarallo, O.; Borbone, F.; Ferone, C.; Colangelo, F.; Catauro, M.; Cioffi, R. Synthesis and characterizations of melamine-based epoxy resins. *Int. J. Mol. Sci.* **2013**, *14*, 18200–18214. [[CrossRef](#)] [[PubMed](#)]
19. Roviello, G.; Ricciotti, L.; Ferone, C.; Colangelo, F.; Cioffi, R.; Tarallo, O. Synthesis and Characterization of Novel Epoxy Geopolymer Hybrid Composites. *Materials* **2013**, *6*, 3943–3962. [[CrossRef](#)] [[PubMed](#)]
20. Chiarella, F.; Barra, M.; Ricciotti, L.; Aloisio, A.; Cassinese, A. Morphology, electrical performance and potentiometry of PDIF-CN2 thin-film transistors on HMDS-treated and bare silicon dioxide. *Electronics* **2014**, *3*, 76–86. [[CrossRef](#)]
21. Colangelo, F.; Roviello, G.; Ricciotti, L.; Ferone, C.; Cioffi, R. Preparation and characterization of new geopolymer-epoxy resin hybrid mortars. *Materials* **2013**, *6*, 2989–3006. [[CrossRef](#)] [[PubMed](#)]

22. Strini, A.; Roviello, G.; Ricciotti, L.; Ferone, C.; Messina, F.; Schiavi, L.; Cioffi, R. TiO<sub>2</sub>-Based Photocatalytic Geopolymers for Nitric Oxide Degradation. *Materials* **2016**, *9*, 513. [[CrossRef](#)] [[PubMed](#)]
23. Roviello, G.; Ricciotti, L.; Ferone, C.; Colangelo, F.; Tarallo, O. Fire resistant melamine based organic-geopolymer hybrid composites. *Cem. Concr. Compos.* **2015**, *59*, 89–99. [[CrossRef](#)]
24. Roviello, G.; Menna, C.; Tarallo, O.; Ricciotti, L.; Ferone, C.; Colangelo, F.; Asprone, D.; di Maggio, R.; Cappelletto, E.; Prota, A.; et al. Preparation, structure and properties of hybrid materials based on geopolymers and polysiloxanes. *Mater. Des.* **2015**, *87*, 82–94. [[CrossRef](#)]
25. Colangelo, F.; Cioffi, R.; Roviello, G.; Capasso, I.; Caputo, D.; Aprea, P.; Liguori, B.; Ferone, C. Thermal cycling stability of fly ash based geopolymer mortars. *Compos. Part B* **2017**, *129*, 11–17. [[CrossRef](#)]
26. Messina, F.; Ferone, C.; Molino, A.; Roviello, G.; Colangelo, F.; Molino, B.; Cioffi, C. Synergistic recycling of calcined clayey sediments and water potabilization sludge as geopolymer precursors: Upscaling from binders to precast paving cement-free bricks. *Constr. Build. Mater.* **2017**, *133*, 14–26. [[CrossRef](#)]
27. Roviello, G.; Menna, C.; Tarallo, O.; Ricciotti, L.; Messina, F.; Ferone, C.; Asprone, D.; Cioffi, R. Lightweight geopolymer-based hybrid materials. *Compos. Part B Eng.* **2017**, *128*, 225–237. [[CrossRef](#)]
28. Colangelo, F.; Roviello, G.; Ricciotti, L.; Ferrándiz-Mas, V.; Messina, F.; Ferone, C.; Tarallo, O.; Cioffi, R.; Cheeseman, C.R. Mechanical and thermal properties of lightweight geopolymer composites containing recycled expanded polystyrene. *Cem. Concr. Compos.* **2018**, *86*, 266–272. [[CrossRef](#)]
29. Roviello, G.; Ricciotti, L.; Tarallo, O.; Ferone, C.; Colangelo, F.; Roviello, V.; Cioffi, R. Innovative fly ash geopolymer-epoxy composites: Preparation, microstructure and mechanical properties. *Materials* **2016**, *9*, 461. [[CrossRef](#)] [[PubMed](#)]
30. Kong, D.L.Y.; Sanjayan, J.G.; Sagoe-Crentsil, K. Comparative performance of geopolymers made with metakaolin and fly ash after exposure to elevated temperatures. *Cem. Concr. Res.* **2007**, *37*, 1583–1589. [[CrossRef](#)]
31. White, C.E.; Provis, J.L.; Proffen, T.; van Deventer, J.S.J. The effects of temperature on the local structure of metakaolin-based geopolymer binder: A neutron pair distribution function investigation. *J. Am. Ceram. Soc.* **2010**, *93*, 3486–3492. [[CrossRef](#)]
32. Duxson, P.; Lukey, G.C.; van Deventer, J.S.J. Physical evolution of Na-geopolymer derived from metakaolin up to 1000 °C. *J. Mater. Sci.* **2007**, *42*, 3044–3054. [[CrossRef](#)]
33. Van Jaarsveld, J.G.S.; van Deventer, J.S.J.; Lukey, G.C. The characterisation of source materials in fly ash-based geopolymers. *Mater. Lett.* **2003**, *57*, 1272–1280. [[CrossRef](#)]
34. Barbosa, V.F.F.; MacKenzie, K.J.D.; Thaumaturgo, C. Synthesis and characterisation of materials based on inorganic polymers of alumina and silica: Sodium polysialate polymers. *Int. J. Inorg. Mater.* **2000**, *2*, 309–317. [[CrossRef](#)]
35. Aronne, A.; Esposito, S.; Ferone, C.; Pansini, M.; Pernice, P. FTIR study of the thermal transformation of barium-exchanged zeolite A to celsian. *J. Mater. Chem.* **2002**, *12*, 3039–3045. [[CrossRef](#)]
36. Ortego, J.D.; Barroeta, Y. Leaching effects on silicate polymerization, A FTIR and <sup>29</sup>Si NMR study of lead and zinc in Portland cement. *Environ. Sci. Technol.* **1991**, *25*, 1171–1174. [[CrossRef](#)]
37. Clayden, N.J.; Esposito, S.; Aronne, A.; Pernice, P. Solid state <sup>27</sup>Al NMR and FTIR study of lanthanum aluminosilicate glasses. *J. Non-Cryst. Solids* **1999**, *258*, 11–19. [[CrossRef](#)]
38. Fellahi, S.; Chikhi, N.; Bakar, M. Modification of epoxy resin with kaolin as a toughening agent. *J. Appl. Polym. Sci.* **2001**, *82*, 861–878. [[CrossRef](#)]
39. Wang, H.; Li, H.; Yan, F. Synthesis and mechanical properties of metakaolinite-based geopolymer. *Colloids Surf. A* **2005**, *268*, 1–6. [[CrossRef](#)]
40. Silverstein, R.M.; Bassler, G.C.; Morrill, T.C. *Spectrometric Identification of Organic Compounds*, 4th ed.; John Wiley and Sons: New York, NY, USA, 1981.
41. Barbosa, V.F.F.; MacKenzie, K.J.D. Thermal behaviour of inorganic geopolymers and composites derived from sodium polysialate. *Mater. Res. Bull.* **2003**, *38*, 319–331. [[CrossRef](#)]

42. Parker, R.W.; Frost, R.L. The application of drift spectroscopy to the multicomponent analysis of organic chemicals adsorbed on montmorillonite. *Clays Clay Miner.* **1996**, *44*, 32–40. [[CrossRef](#)]
43. Frost, R.L.; Fredericks, P.M.; Shurvell, H.F. Raman microscopy of some kaolinite clay minerals. *Can. J. Appl. Spectrosc.* **1996**, *41*, 10–14.



© 2017 by the authors. Licensee MDPI, Basel, Switzerland. This article is an open access article distributed under the terms and conditions of the Creative Commons Attribution (CC BY) license (<http://creativecommons.org/licenses/by/4.0/>).